ELSEVIER

Journal of Hazardous Materials B90 (2002) 77–95

Journal of Hazardous Materials

www.elsevier.com/locate/jhazmat

Removal of copper from aqueous solution by chitosan in prawn shell: adsorption equilibrium and kinetics

K.H. Chu*

School of Engineering and Science, Swinburne University of Technology, P.O. Box 218, Hawthorn, Victoria 3122, Australia

Received 15 April 2001; received in revised form 31 August 2001; accepted 4 September 2001

Abstract

The metal removal capability of prawn shell is evaluated in this study using copper as a model sorbate. A mild deacetylation method was used to convert chitin on the periphery of the shell to chitosan. The equilibrium and kinetic characteristics of copper adsorption on partially deacetylated prawn shell are studied in batch stirred-tank experiments. The extent of copper removal increases with an increase in pH. Both the Langmuir model with pH-dependent parameters and the extended Langmuir–Freundlich model with pH-independent parameters account very well for the measured equilibrium data. Modeling studies using two different second order surface reaction models demonstrate that transient profiles obtained experimentally for a range of initial metal concentrations (C_0) and adsorbent dosage are in good agreement with calculated curves of both models. The two rate models can be used for an accurate description of measured kinetic data so long as their rate constants are properly correlated with the two system variables. In contrast, deviation exists between experimental data and theoretical curves calculated from a diffusion-based model.

Keywords: Adsorption; Chitosan; Heavy metals; Crustacean shell; Kinetics

1. Introduction

Toxic metal ions in trace quantities are difficult to remove from aqueous solutions. Adsorption is one of the few alternatives available for such situations. In recent years, numerous low cost adsorbent materials have been evaluated for their capacity to remove toxic metal ions, as documented in a recent review [1]. These novel adsorbents include a wide range

* Tel.: +61-3-92148028; fax: +61-3-92148264.
E-mail address: kchu@swin.edu.au (K.H. Chu).

0304-3894/02/$ – see front matter
PII: S0304-3894(01)00332-6

Nomenclature

a	parameter defined in Eq. (9) (mmol/g)
A	adsorption site on adsorbent surface
b	parameter defined in Eq. (10) (mmol/g)
C_0	initial metal concentration of solution phase (mmol/l)
C_t	metal concentration in the solution phase at time t (mmol/l)
C_∞	metal concentration of solution phase at equilibrium (mmol/l)
$C_{\infty,\mathrm{H}}$	proton concentration of solution phase at equilibrium (mmol/l)
D_e	effective intra-particle diffusion coefficient (cm^2/min)
h	parameter defined in Eq. (15) (mmol/l)
k_1	forward rate constant of second order reversible reaction model (l/mmol min)
k_{-1}	backward rate constant of second order reversible reaction model (per min)
k_2	rate constant of second order irreversible reaction model (l/mmol min)
K_d	Langmuir apparent dissociation constant for copper (mmol/l)
$K_{\mathrm{d,H}}$	Langmuir apparent dissociation constant for proton (mmol/l)
l	half-thickness of the prawn shell particle (cm)
m	mass of adsorbent (g)
M	metal ion in the solution phase
MA	metal-adsorbent complex
M_t	amount of metal adsorbed at time t (mmol)
M_∞	amount of metal adsorbed at equilibrium (mmol)
n	Langmuir–Freundlich exponent for copper
n_H	Langmuir–Freundlich exponent for proton
q_m	maximum capacity of the adsorbent (mmol/g)
q_t	metal concentration in the adsorbent phase at time t (mmol/g)
q_∞	metal concentration of adsorbent phase at equilibrium (mmol/g)
t	time (min)
v	volume of solution (l)

Greek letters

α	parameter defined in Eq. (20)
β_i	nonzero roots of Eq. (19)

of materials ranging from microbial biomass to by-products derived from industrial, agricultural, and fishery wastes. Recent investigations have shown that crustacean shells, a by-product of the shellfish processing industry, exhibit surface binding specificity toward a range of heavy metal ions [2–5]. The metal ion binding ability of crustacean shell is attributed to the presence of chitin and its deacetylated derivative chitosan in its exoskeletons. The processing waste of crustacean shells contains approximately 10–55% of chitin on a dry weight basis, depending on the method of processing. Chitin, a homopolymer comprising β-(1–4)-linked *N*-acetyl-D-glucosamine residues, is the second most abundant and renewable natural biopolymer. Chitosan is prepared from chitin by deacetylation with

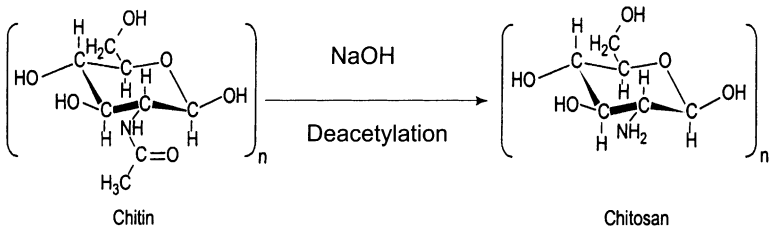

Fig. 1. Conversion of chitin to chitosan by deacetylation.

a strong alkaline solution (Fig. 1). It is a highly versatile molecule with commercial applications in a wide range of areas ranging from water treatment to personal care products. Commercial production of chitosan from the shells of crabs and shrimps in Japan accounts for ∼90% of the global chitosan market [6].

Numerous studies have demonstrated the effectiveness of chitosan and derived products in the uptake of metal cations such as lead, cadmium, copper, and nickel and the uptake of oxyanions as well as complexed metal ions [2–19]. The binding ability of chitosan for metal cations is mainly due to the amine groups ($-NH_2$) on the chitosan chain which can serve as coordination sites for many metals (Fig. 1). The extent of metal adsorption depends on the source of chitosan, the degree of deacetylation, the nature of the metal ion, and solution conditions such as pH. The metal binding process is thus largely unpredictable, which makes experimental procedures the only means of evaluating the metal adsorption property of chitosan. In this work, the metal removal capability of prawn shell is evaluated using copper as a model metal. Nearly 35% of shrimps/prawns are discarded as waste when processed into headless shell-on products. The peeling process, which involves removal of the shell from the tail of the prawn, increases the waste production up to 40–45%. Such waste produced at large-scale processing facilities serves as a reliable and regular source of high quality chitinous material. To enhance the metal removal capability of prawn shell, a relatively mild deacetylation method was used to convert chitin on the periphery of the shell to chitosan.

2. Materials and methods

2.1. Partial deacetylation of chitin in prawn shell

The deacetylation method of Coughlin et al. [2] was used in this work to convert chitin on the periphery of prawn shell (*Penaeus monodon*) to its deacetylated derivative, chitosan. The shell was washed under running water, followed by rinsing with distilled water and drying overnight at 60 °C. The dried shell was ground in a blender and sieved. Shell particles in the size range 0.5–1.0 mm were first soaked in a 5% hydrochloric acid solution for 1 h at room temperature to remove calcium salts (demineralization). After rinsing with distilled water, a portion of the decalcified prawn shell was transferred to a 50% sodium hydroxide solution and incubated in a shaker at 90 °C for 1 h for partial deacetylation. After rinsing

with distilled water and drying at 60 °C, the deacetylated shell particles were ready for use in copper adsorption experiments.

2.2. Equilibrium uptake experiments

Batch equilibrium experiments were carried out using partially deacetylated prawn shell as well as decalcified prawn shell as adsorbents. A series of flasks containing copper solutions of varying concentrations prepared from copper sulfate salt (Fluka, Switzerland) and a fixed dosage of prawn shell (5 g/l) were agitated in a rotary shaker at 200 rpm, 25 °C for 24 h which was sufficient for the copper uptake process to reach equilibrium. Copper uptake experiments were conducted under constant pH values of 3, 4, 5, and 6 by adding sulfuric acid or sodium hydroxide as required. After equilibration, the copper solutions were filtered through 0.45 μm membrane filters, acidified and analyzed for copper content by an inductively coupled plasma spectrometer (ICP 2000, Baird, USA). Copper-free and adsorbent-free blanks were used as controls. Amounts of copper taken up by the adsorbent in each flask were determined by the following mass balance equation:

$$q_\infty = \frac{v}{m}(C_0 - C_\infty) \tag{1}$$

where q_∞ and C_∞ are respectively the adsorbent phase metal concentration and solution phase metal concentration at equilibrium; C_0, the initial metal concentration; v, the solution volume, and m is the mass of adsorbent.

2.3. Transient uptake experiments

Batch experiments for determination of the kinetics of copper adsorption on prawn shell were carried out using a continuously stirred glass vessel with a diameter of 12.7 cm and a height of 24 cm. A motor was used to drive two 6-blade Rushton turbine impellers with a diameter of 4.5 cm. Three baffles were spaced evenly around the vessel. The following experimental conditions were kept constant for the kinetic experiments: volume of solution = 1 l; temperature = 25 °C; pH = 6; and stirring speed = 300 rpm, to fully suspend and uniformly disperse the adsorbent particles in the solution. Two main system variables, C_0 and adsorbent dosage, were varied to investigate their effect on the adsorption kinetics. During the kinetic experiments, samples were withdrawn at fixed time intervals, filtered, acidified and analyzed for copper as described above.

3. Results and discussion

Many of the methods reported for converting chitin in crustacean shell to chitosan are slow and consume significant amounts of reagents. A relatively rapid and mild deacetylation method proposed by Coughlin et al. [2] was used in this work to develop chitosan on the exterior surface of prawn shell without substantially converting the interior region of the shell. It has been demonstrated that metal uptake by crab shell treated by this method was confined to the outer surface of the shell in batch studies with contact times as long as

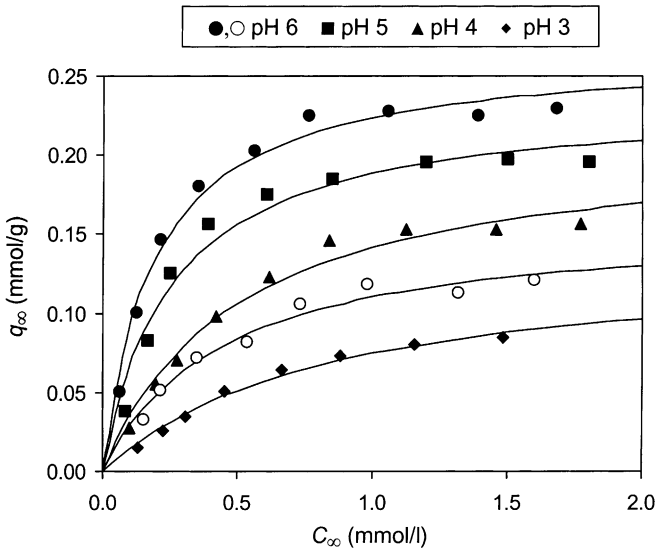

Fig. 2. Effect of pH on adsorption equilibria of copper on deacetylated prawn shell (solid symbols) and decalcified prawn shell (open symbols); lines: Langmuir model fits.

12 h [2]. The metal ion removal ability of partially converted shell is thus similar to that of more exhaustively deacetylated material whose interior binding sites are most likely not accessible to metal ions in experiments with contact times of several hours.

Equilibrium data for copper adsorption on partially deacetylated prawn shell at different pH values as well as on decalcified prawn shell at pH 6 are shown as symbols in Fig. 2. It is evident that copper uptake by partially deacetylated prawn shell is higher than that of decalcified prawn shell at the same pH over the entire range of solution phase concentration examined in this study, demonstrating the beneficial effect of deacetylation. In general, copper uptake by partially deacetylated prawn shell increases approximately linearly with pH within the range of 3–6. This adsorption trend can likely be ascribed to the effect of competitive binding between copper ions which exist as Cu^{2+} under the experimental conditions [20] and protons for the finite number of amine groups in chitosan. X-ray photoelectron spectroscopic studies have confirmed that the amine groups are largely responsible for the sequestration of copper ions from solution [21]. At low solution pH, the amine groups are protonated to varying degrees, reducing the number of binding sites available for copper uptake. As a result, the extent of copper uptake is low in the presence of high concentrations of protons.

Relatively simple isotherm models such as the Langmuir model often provides an adequate description of metal adsorption equilibria on a wide range of adsorbent materials. The Langmuir equation is defined as follows:

$$q_\infty = \frac{q_m C_\infty}{K_d + C_\infty} \tag{2}$$

Table 1
Best-fit Langmuir parameters for copper adsorption on partially deacetylated prawn shell

	pH			
	3	4	5	6
q_m (mmol/g)	0.137	0.212	0.236	0.266 (0.159)[a]
K_d (mmol/l)	0.842	0.500	0.254	0.189 (0.446)
r^2	0.991	0.985	0.978	0.988 (0.983)

[a] Values in brackets refer to copper adsorption on decalcified prawn shell.

where q_m is the pH-dependent maximum adsorption capacity and K_d is the pH-dependent apparent dissociation constant. Eq. (2) was fitted to each set of the equilibrium data by a non-linear least-squares regression analysis. Regressed values of the model parameters q_m and K_d along with values of the regression coefficient r^2 are listed in Table 1. The best-fit isotherms obtained from Eq. (2) are shown as solid lines in Fig. 2. In general, the experimental data are well represented by the Langmuir model.

Owing to its prevalent use in the research community, the Langmuir model has become a useful and convenient tool for comparing the adsorption properties of different adsorbents. Table 2 lists selected values of q_m and K_d for copper adsorption on various types of chitosan, along with the q_m and K_d values for the partially deacetylated prawn shell used in this study. As expected, the q_m of the partially converted prawn shell for copper is smaller than those of relatively pure chitosan extracted from various crustacean shells. The K_d for the prawn shell falls within the range of values quoted in Table 2. A small K_d value is desired since it indicates a steep initial slope of an isotherm, which in turn implies a high affinity of the adsorbent for the sorbate under dilute conditions. Although the adsorption capacity of the prawn shell is lower than that of relatively pure chitosan, it is a cost competitive adsorbent material owing to the relatively low cost of preparation. Because the cost of obtaining partially converted prawn shell is likely to be strongly influenced by the costs of prawn shell collection and delivery, no detailed cost estimation of prawn shell preparation can be made without reference to specific cases. Nevertheless, an approximate economic comparison of a batch process based on sorption on partially converted crab shell to the conventional precipitation process indicated that the former was more cost effective for treatment of a typical metal-bearing waste stream generated by a small electroplating firm [2].

Although the Langmuir model can provide an adequate description of convex adsorption isotherms, the model does not incorporate pH effects. In other words, the Langmuir para-

Table 2
K_d and q_m for copper of selected chitosan adsorbents

Adsorbent	pH	q_m (mmol/g)	K_d (mmol/l)	Source
Crosslinked chitosan beads	5	3.91	4.14	[7]
Chitosan flakes	4.7–5.4	2.75	0.26	[8]
Chitosan powder	5	0.71	0.03	[9]
Chitosan flakes	6	0.33	0.03	[10]
Prawn shell	6	0.27	0.19	This work

Table 3
Best-fit parameters for the extended Langmuir model and extended Langmuir–Freundlich model

	Extended Langmuir	Extended Langmuir–Freundlich
q_m (mmol/g)	0.241	0.246
K_d (mmol/l)	0.183	0.087
$K_{d,H}$ (mmol/l)	0.053	0.041
n	–	0.960
n_H	–	1.881

meters q_m and K_d are pH-dependent and each set of q_m and K_d is only valid for one particular pH value. Since proton competes with copper for binding sites on the prawn shell, a simple approach to incorporate the effect of pH within the Langmuir model is to extend the model to account for the uptake of both copper and proton. Such an approach yields the following binary isotherm model for copper, commonly known as the extended Langmuir model or the competitive Langmuir model [22]:

$$q_\infty = \frac{q_m C_\infty}{K_d + C_\infty + (K_d/K_{d,H})C_{\infty,H}} \tag{3}$$

where $C_{\infty,H}$ is the proton concentration in the solution phase at equilibrium and $K_{d,H}$ is the apparent dissociation constant for proton. Eq. (3) was fitted empirically to the entire set of equilibrium data in Fig. 2 by a non-linear regression analysis to determine the best values of the three parameters q_m, K_d, and $K_{d,H}$. The fitted parameters are listed in Table 3. The fits of the extended Langmuir model are shown as solid lines in Fig. 3a, where they are compared with the experimental equilibrium isotherms (symbols). It is obvious that the extended Langmuir equation with three best-fit parameters has been found inadequate to accurately correlate all experimental equilibrium isotherms in Fig. 2.

The correlative capability of the extended Langmuir model may be enhanced by the introduction of a power law of the Freundlich form:

$$q_\infty = \frac{q_m C_\infty^{1/n}}{K_d + C_\infty^{1/n} + (K_d/K_{d,H})C_{\infty,H}^{1/n_H}} \tag{4}$$

where n and n_H are the Langmuir–Freundlich exponents for copper and proton, respectively. Eq. (4), commonly called the extended Langmuir–Freundlich isotherm, was fitted to the equilibrium data in Fig. 2. The agreement between each equilibrium data set and model fit is very good, as shown in Fig. 3b. This is not surprising as the extended Langmuir–Freundlich equation with five adjustable parameters has greater flexibility in fitting experimental data than the extended Langmuir equation with three adjustable parameters. Best-fit values of the five parameters are summarized in Table 3. These pH-independent parameters can be used to predict equilibrium isotherms at any pH within the range of 3–6.

In addition to equilibrium data, information on adsorption kinetics is required for a comprehensive analysis of batch systems. The effects of two main system variables, C_0 and adsorbent dosage, on the transient behavior of copper removal by prawn shell were examined owing to their practical importance. Experimental transient profiles of copper removal in

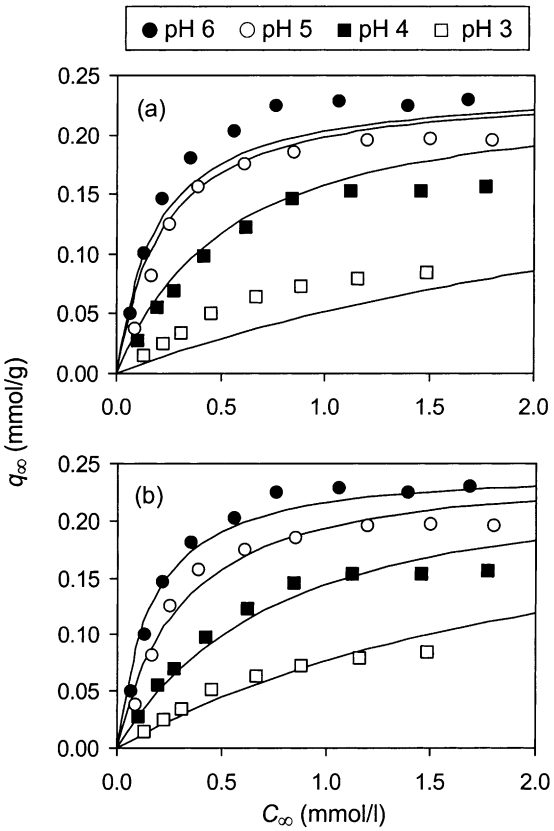

Fig. 3. Effect of pH on adsorption equilibria of copper on deacetylated prawn shell. Symbols: experimental data; lines: model fits using (a) extended Langmuir model and (b) extended Langmuir–Freundlich model.

the stirred batch apparatus obtained at different C_0s are shown as symbols in Fig. 4a. The pH and adsorbent dosage for these experiments were fixed at 6 and 5 g/l, respectively. The concentration decay profiles of the solution phase in Fig. 4a are reported in terms of the ratio C_t/C_0, where C_t is the measured solution phase metal concentration at time t. The experimental C_t/C_0 curves approached higher asymptotic values with the increase in C_0. This trend is expected for a batch contactor with a fixed adsorbent dosage and varying C_0, since the fraction of metal removed from the aqueous phase becomes smaller as the C_0 is increased. The rate of adsorption generally depends on the C_0. An increase in C_0 resulted in an increase in the contact time needed to reach apparent equilibrium.

The effect of adsorbent dosage on the adsorption kinetics is shown in Fig. 4b (symbols). For these experiments, $C_0 = 50$ mg/l and pH $= 6$. The adsorption trends in these experiments are opposite to those observed in the C_0 experiments. Firstly, the experimental C_t/C_0 curves approached lower asymptotic values with the increase in adsorbent dosage. This trend is again expected for a batch contactor with a fixed C_0 and varying adsorbent

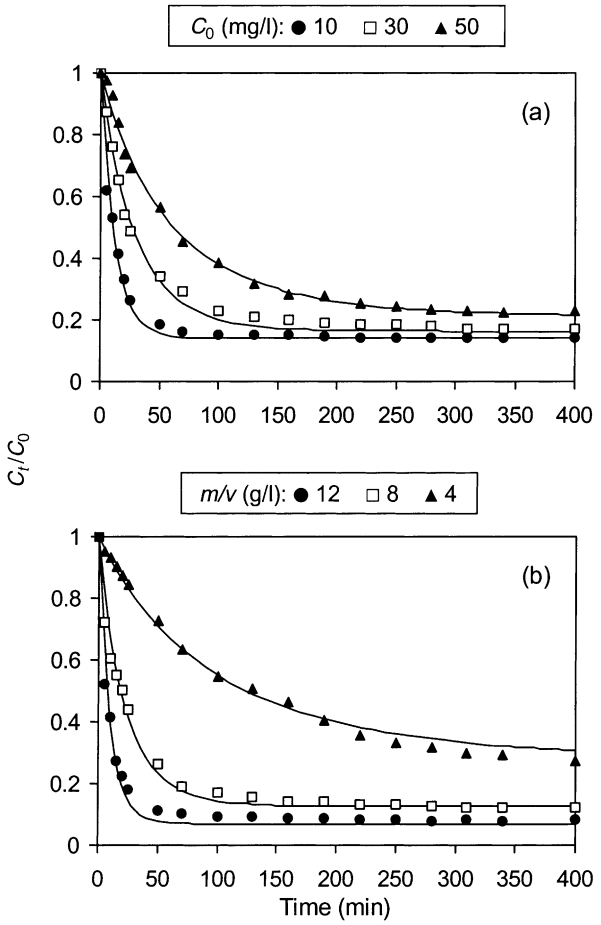

Fig. 4. Copper concentration decay profiles of the solution phase. (a) Effect of C_0; (b) effect of adsorbent dosage (m/v). Symbols: experimental data; lines: second order reversible reaction model fits.

dosage because the fraction of metal removed from the aqueous phase becomes bigger as the adsorbent dosage is increased. Secondly, an increase in the adsorbent dosage resulted in a decrease in the contact time required to reach apparent equilibrium.

Mathematical models are useful for interpreting the observed effects of C_0 and adsorbent dosage on the adsorption kinetics. Numerous mathematical models with varying degrees of complexity have been developed for metal adsorption in batch systems [23]. Most of these models, which may include surface reaction kinetics as well as various steps of mass transfer resistance, have originated mainly from the research on metal adsorption to porous, spherical activated carbon and ion exchange resins. Use of these models to describe metal adsorption by non-conventional adsorbents is somewhat cumbersome because most of these adsorbents, including the prawn shell used in this study, are sheet-like and of

irregular shape. Since copper uptake is expected to be largely limited to the exterior surface of the prawn shell owing to the partial deacetylation method used here, we examined the capability of two surface reaction models, namely a second order reversible reaction model and a second order irreversible reaction model, for describing copper removal by prawn shell.

In the second order reversible reaction model, it is assumed that the interaction that occurs between a metal ion and the binding site at the adsorbent surface may be represented by a reversible reaction of the form

$$M + A \underset{k_{-1}}{\overset{k_1}{\rightleftarrows}} \mathrm{MA} \tag{5}$$

where M is the metal ion in solution, A is the adsorption site and MA is the metal-adsorbent complex. The parameters k_1 and k_{-1} are the second order forward and first order reverse rate constants, respectively. The rate of metal uptake by the adsorbent in an interaction described by Eq. (5) is given by

$$\frac{\mathrm{d}q_t}{\mathrm{d}t} = k_1 C_t (q_\mathrm{m} - q_t) - k_{-1} q_t \tag{6}$$

where q_t and C_t are respectively the adsorbent phase metal concentration and solution phase metal concentration at time t. At equilibrium, Eq. (6) reduces to the Langmuir isotherm equation (Eq. (2)) where K_d is given by

$$K_\mathrm{d} = \frac{k_{-1}}{k_1} \tag{7}$$

The extent of metal ion uptake as a function of time can be found from the integration of Eq. (6) together with the appropriate initial conditions and the mass balance equation for a batch system. The analytic solution of Eq. (6) is given by [24]

$$\frac{C_t}{C_0} = 1 - \frac{1}{C_0}\frac{m}{v}\frac{(b+a)[1-\exp(-2a(m/v)k_1 t)]}{[((b+a)/(b-a)) - \exp(-2a(m/v)k_1 t)]} \tag{8}$$

where the parameters a and b are defined as

$$a^2 = b^2 - C_0 q_\mathrm{m}\frac{v}{m} \tag{9}$$

$$b = 0.5\left(C_0\frac{v}{m} + q_\mathrm{m} + K_\mathrm{d}\frac{v}{m}\right) \tag{10}$$

Alternatively, the interaction that occurs between a metal ion and the adsorbent may be represented by a second order irreversible reaction of the form

$$M + A \overset{k_2}{\rightarrow} \mathrm{MA} \tag{11}$$

where k_2 is the second order rate constant. The rate of change of solution phase metal concentration in an interaction described by Eq. (11) is given by [25]

$$\frac{\mathrm{d}C_t}{\mathrm{d}t} = -k_2 C_t (C_t - C_\infty) \tag{12}$$

The analytic solution of Eq. (12) can be found by integration with the appropriate initial conditions and is given by

$$\frac{C_t}{C_0} = \frac{C_\infty}{C_0 - (C_0 - C_\infty)\exp(-C_\infty k_2 t)} \tag{13}$$

When the equilibrium relationship of the adsorption system is of Langmuir form, C_∞ for a batch system is given by

$$C_\infty = \frac{-h + \sqrt{h^2 + 4C_0 K_d}}{2} \tag{14}$$

where the parameter h is defined as

$$h = K_d - C_0 + q_m \frac{m}{v} \tag{15}$$

Note that K_d in this case is no longer defined by Eq. (7) and is treated as an empirical parameter that correlates the adsorption equilibrium.

The experimental transient profiles in Fig. 4 are compared with solutions of the two models according to the relationships established in Eqs. (8) and (13) to extract the values of the respective surface interaction rate constants k_1 and k_2. Values of k_1 and k_2, tabulated in Table 4, were estimated by fitting Eqs. (8) and (13) to the measured concentration decay profiles by a non-linear least-squares regression analysis. The fitting begins with an estimation of the value of k_1 or k_2 and then keeps optimizing its value until the sum of squared residuals no longer decreases significantly. It should be noted that each model contains only one adjustable parameter (k_1 or k_2). Other parameters associated with Eqs. (8)–(10) and (13)–(15) are either known (C_0, m, and v) or have been determined previously (q_m and K_d). Note that the value of k_{-1} for the second order reversible reaction model can be readily calculated from Eq. (7) once k_1 is known. Concentration decay curves calculated by the second order reversible and irreversible models are shown as solid lines in Figs. 4 and 5, respectively, in comparison with the measured data. A satisfactory fit is obtained between the calculated and experimental transient profiles for all experiments. There is essentially no difference in the ability of the two models to accurately fit the measured data. It is generally difficult to distinguish among kinetic models on the basis of how well they fit measured data, as models based on different assumptions can often provide

Table 4
Best-fit rate constants k_1 and k_2

Experimental conditions		k_1 (l/mmol min)	k_2 (l/mmol min)
C_0 (mg/l)	Adsorbent dosage (g/l)		
10	5	0.055	0.856
30	5	0.023	0.109
50	5	0.011	0.031
50	4	0.008	0.018
50	8	0.021	0.091
50	12	0.034	0.253

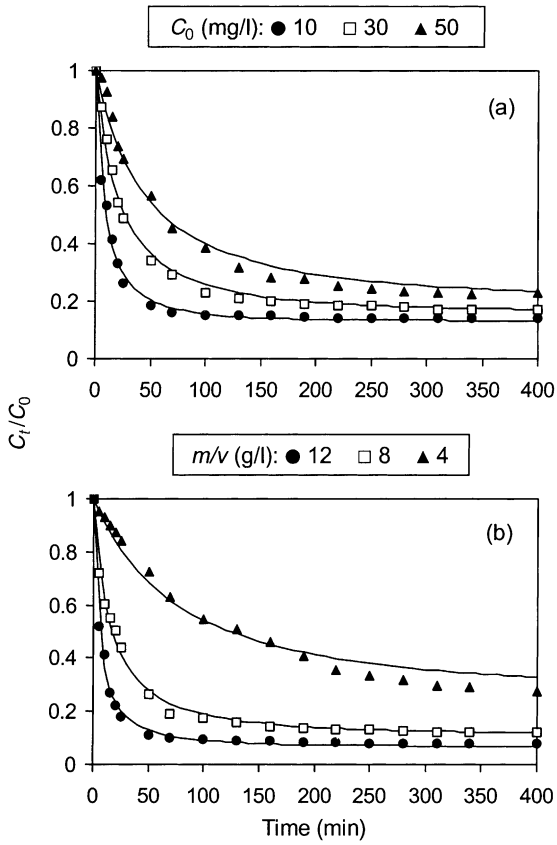

Fig. 5. Copper concentration decay profiles of the solution phase. (a) Effect of C_0; (b) effect of adsorbent dosage (m/v). Symbols: experimental data; lines: second order irreversible reaction model fits.

nearly identical fits, as observed in this study. Discrimination between the two models requires more fundamental studies of the adsorption process than afforded by interpretation of observed rates.

As may be seen from Table 4, it is not possible to fit the entire data set with a single value of k_1 or k_2. To discern the relationships between the rate constants and C_0/adsorbent dosage, the best-fit values of k_1 and k_2 listed in Table 4 are plotted against the two system variables, as shown in Figs. 6 and 7. It appears that both k_1 and k_2 increase with a decrease in C_0 and an increase in adsorbent dosage.

The observed dependence of the surface interaction rate constants on C_0 and adsorbent dosage may be attributed to the effect of heterogeneous binding. The equilibrium results in Fig. 2 indicate that decalcified prawn shell containing mainly chitin is capable of sequestering an appreciable amount of copper from aqueous solution. It is reasonable to assume that partially deacetylated prawn shell offers both chitosan and unconverted chitin as

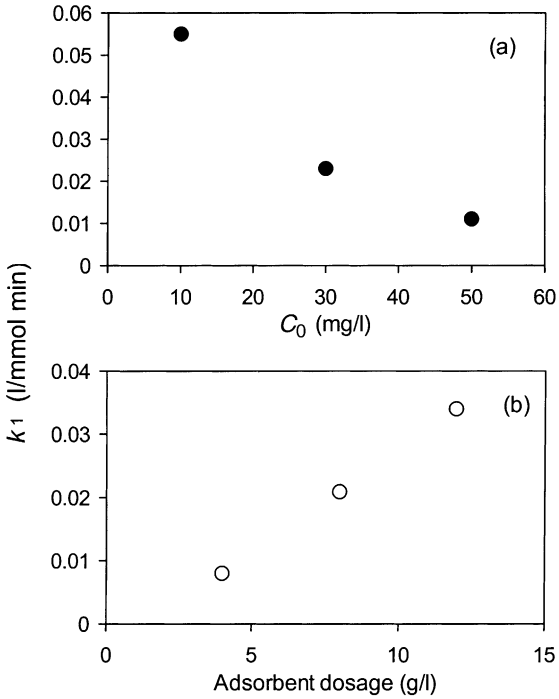

Fig. 6. Variation of rate constant k_1 with (a) C_0 and (b) adsorbent dosage.

potential binding sites for copper with chitosan being the high energy site. Copper binding to these high energy sites is assumed to be characterized by fast reaction kinetics. In a batch contactor, a low metal loading environment is crated by using a low C_0 at a fixed adsorbent dosage or a high adsorbent dosage at a fixed C_0. Under such conditions the metal will bind preferentially to high energy sites. This is because sites of highest energy are usually taken up by sorbate first and then sites of lower energy are progressively filled as the metal loading is increased. It follows that copper binding in low metal loading experiments (low C_0 or high adsorbent loading) will result in higher $k_1$and k_2 values, reflecting fast reaction kinetics for copper binding to chitosan. On the other hand, copper binding in high metal loading experiments (high C_0 or low adsorbent dosage) will yield lower average k_1 and k_2 values because some of the copper ions are sorbed to lower energy sites (chitin). The effects of C_0 and adsorbent dosage on the rate constants can therefore be explained in terms of the degree of metal loading on the adsorbent.

Fig. 8 shows the relationships between the rate constants and metal loading which is reported in terms of percent metal loading ($100\% \times q_\infty / q_\mathrm{m}$). The value of q_∞ was calculated for each transient curve from the mass balance equation (Eq. (1)) using the experimental asymptotic C_t values in Fig. 4 for C_∞ in Eq. (1) and the appropriate C_0, v, and m values. A direct correlation between the rate constants and metal loading can now be established. The following empirical equations relating k_1 and k_2 to metal loading have been obtained

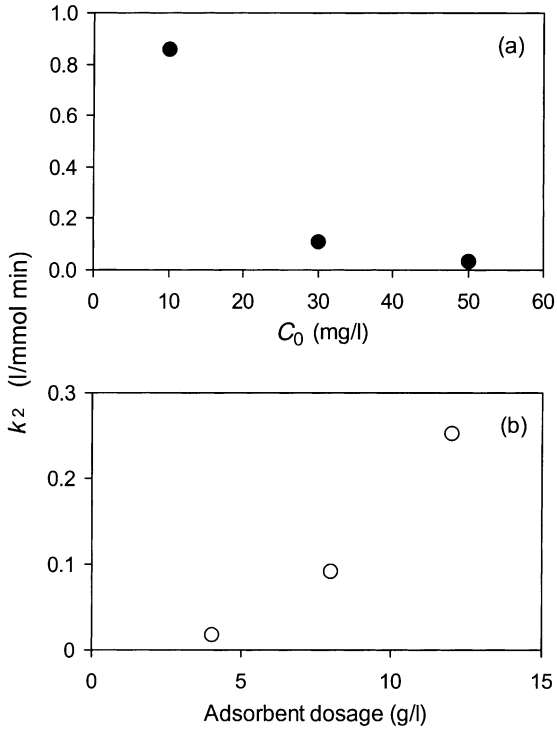

Fig. 7. Variation of rate constant k_2 with (a) C_0 and (b) adsorbent dosage.

by a non-linear regression of the data in Fig. 8:

$$k_1 = 0.087 \exp[-0.044(\text{percent metal loading})] \tag{16}$$

$$k_2 = 2.367 \exp[-0.1(\text{percent metal loading})] \tag{17}$$

The solid lines in Fig. 8, obtained from Eqs. (16) and (17), indicate that the non-linear equations are adequate for correlating the data. The hypothesis can thus combine the effects of two system variables (C_0 and adsorbent dosage) on rate constants into a single system parameter: metal loading on the adsorbent.

In the preceding analysis the intrinsic sorption kinetics has been regarded as rate controlling with all other rate processes assumed to be essentially at equilibrium. The overall rate of adsorption in a typical porous adsorbent such as activated carbon is generally controlled by mass transfer resistance rather than by the intrinsic kinetics of sorption at the surface. However, the rate-limiting process in non-conventional adsorbents with different physical properties, particle geometry, and binding mechanisms is not always immediately obvious. It is therefore of interest to examine the relative importance of mass transfer resistance and intrinsic sorption kinetics for the prawn shell adsorbent used in this study. Porous adsorbents offer two distinct resistances to mass transfer: external film diffusion associated with

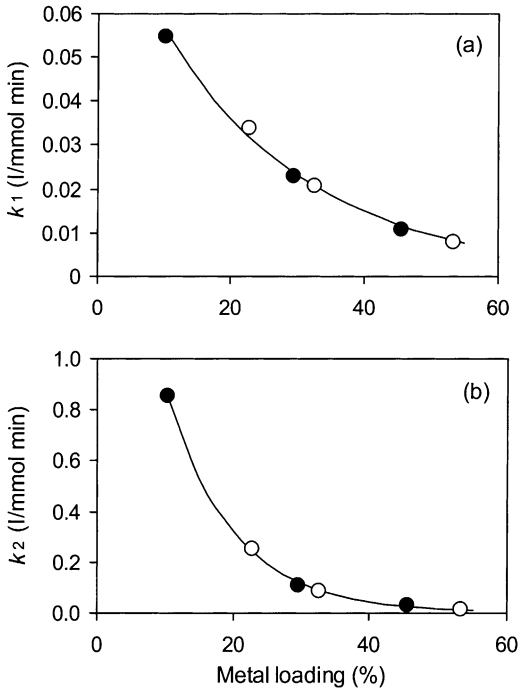

Fig. 8. (a) Variation of rate constant k_1 with percent metal loading. Solid symbols: data from Fig. 6a. Open symbols: data from Fig. 6b. Line: prediction obtained from Eq. (16). (b) Variation of rate constant k_2 with percent metal loading. Solid symbols: data from Fig. 7a. Open symbols: data from Fig. 7b. Line: prediction obtained from Eq. (17).

transport through the laminar fluid boundary layer surrounding the particle and intra-particle transport which may occur by several different diffusive mechanisms [22].

The usual test of varying the agitation speed in a batch vessel to confirm the absence of significant external resistance was carried out. The results indicate that after the agitation rate increased beyond 200 rpm the resulting transient profiles of the copper concentration in the bulk solution agreed with each other within about 3% error (data not shown). Since the agitation rate was set at 300 rpm for all kinetic experiments reported in this study, the effect of the film mass transfer resistance has been eliminated through adequate turbulence created by proper agitation in the batch vessel.

To investigate the role of intra-particle diffusion we checked the conformity of the experimental data with theoretical predictions calculated from an appropriate diffusion model for the prawn shell adsorbent. For the relatively flat prawn shell particle, the thickness of the particle is much smaller than the length and width. The prawn shell particle can thus be considered as a thin plate rather than a spherical particle with intra-particle diffusion occurring in the thickness direction. Assuming intra-particle diffusion control and a linear equilibrium relation analytic solutions have been derived for a one-dimensional plate diffusion model for an infinitely large volume system and a finite volume system [26]. The

latter solution is the practically important solution for the analysis of uptake curves for experimental liquid phase systems in which the sorption curve is followed by monitoring the liquid phase concentration. The expression for the uptake rate in a finite volume system in which uptake into a parallel-sided adsorbent slab is controlled entirely by intra-particle diffusion is given below in the form of an infinite series [26]:

$$\frac{M_t}{M_\infty} = 1 - \sum_{i=1}^{\infty} \frac{2\alpha(1+\alpha)}{1+\alpha+\alpha^2\beta_i^2} \exp\left(-\frac{\beta_i^2 D_e t}{l^2}\right) \tag{18}$$

where M_t and M_∞ are the amount of metal adsorbed at time t and at equilibrium, respectively; l, the half-thickness of the prawn shell particle, and D_e is the effective intra-particle diffusion coefficient. The parameter β_i is given by the positive, nonzero roots of the equation

$$\tan\beta_i = -\alpha\beta_i \tag{19}$$

and the parameter α is expressed in terms of the final fractional uptake of metal by the adsorbent slab by the relation

$$\frac{M_\infty}{vC_0} = \frac{C_0 - C_\infty}{C_0} = \frac{1}{1+\alpha} \tag{20}$$

For most values of α a more useful and convenient form of Eq. (18) is given by

$$\frac{M_t}{M_\infty} = (1+\alpha)\left(1 - \exp\left(\frac{D_e t}{l^2\alpha^2}\right) \operatorname{erfc}\sqrt{\frac{D_e t}{l^2\alpha}}\right) \tag{21}$$

Eq. (21) provides the basis for analysis of transient uptake curves for sorption in flat sheets for which the uptake rate is controlled entirely by intra-particle diffusion.

Of the three model parameters of Eq. (21), l (0.01 cm) could be measured directly and α (0.163) could be calculated from Eq. (20) once the initial and final concentrations of the metal solution in the batch vessel are known. This means that Eq. (21) will give a specific theoretical uptake profile for a specific value of the third parameter, D_e. A family of theoretical uptake curves, calculated according to Eq. (21) with D_e in the range (1–4)10^{-7} cm^2/min, to simulate uptake under the experimental conditions corresponding to the case of $C_0 = 10$ mg/l (Table 4) is shown in Fig. 9. Under these conditions, the uptake rate was measured over the linear region of the equilibrium isotherm for pH 6, as may be seen from Fig. 2. Fig. 9 provides a simple means of checking the conformity of the experimental data with the diffusion equation. As expected, the larger is D_e, the sooner the system approaches equilibrium. It is evident that the shape of the experimental uptake curve differs from the theoretical curves for intra-particle diffusion control. The fractional approach to equilibrium calculated with $D_e = 1 \times 10^{-7}$ cm^2/min fitted the experimental data well in the initial region ($t < 10$ min) but under-predicted uptake at $t > 10$ min while the theoretical curve calculated with $D_e = 2 \times 10^{-7}$ cm^2/min over-predicted uptake at short times and under-predicted uptake in the long time region. Uptake curves calculated with $D_e = 3$ and 4×10^{-7} cm^2/min or larger (not shown) predicted the measured data well at long times but over-predicted uptake at short times. The poor conformity of the model prediction with measured data may therefore be regarded as strong circumstantial evidence that the diffusion-based model does not mechanistically describe the uptake process. This

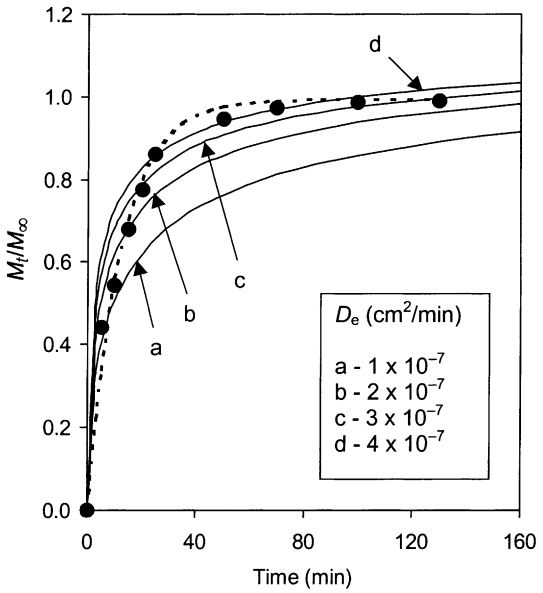

Fig. 9. Experimental and theoretical copper uptake profiles of the adsorbent phase. Symbols: experimental data with $C_0 = 10$ mg/l and $m/v = 5$ g/l. Solid lines: predictions calculated from the diffusion model, Eq. (21). Dashed line: prediction calculated from the second order reversible reaction model, Eq. (22).

is probably due to the fact that copper uptake was mainly confined to the exterior surface of the partially deacetylated prawn shell with very little copper distribution within the interior region. Using energy dispersive X-ray analysis Coughlin et al. [2] were able to show high concentration of sorbed nickel at the surface of crab shell and very low concentration of nickel in the interior region, providing direct physical evidence on negligible penetration of metal ions in partially converted crab shell. Those experimental observations together with the simulation results reported here seem to suggest that diffusional distances for metal transport in partially deacetylated crustacean shell are shallow, although we have not verified this fact experimentally in the case of prawn shell.

It is of interest to assess the ability of the two reaction-based models to simulate the uptake curve shown in Fig. 9 using the best-fit rate constants listed in Table 4. Uptake curves can be calculated from the two reaction rate models (Eqs. (8) and (13)) using the corresponding expressions for metal uptake in the adsorbent phase:

Second order reversible reaction model:

$$\frac{M_t}{M_\infty} = \frac{q_t}{q_\infty} = \frac{m}{v(C_0 - C_\infty)} \frac{(b+a)[1 - \exp(-2a(m/v)k_1 t)]}{[((b+a)/(b-a)) - \exp(-2a(m/v)k_1 t)]} \tag{22}$$

Second order irreversible reaction model:

$$\frac{M_t}{M_\infty} = \frac{q_t}{q_\infty} = \frac{C_0}{C_0 - C_\infty} \left(1 - \frac{C_\infty}{C_0 - (C_0 - C_\infty)\exp(-C_\infty k_2 t)}\right) \tag{23}$$

As expected, the form of the experimental uptake curve is quantitatively predicted by the second order reversible reaction model (Eq. (22)) throughout the whole time course of uptake, as shown in Fig. 9 (dashed line). The prediction of the irreversible reaction model (Eq. (23)) closely mirrored that of the reversible reaction model (not shown). For the copper–prawn shell system the assumption that mass transfer effects are unimportant and intrinsic sorption kinetics associated with metal ion binding mechanisms such as chelation and ion exchange is rate controlling thus appears to be justified.

4. Conclusion

Equilibrium and transient data for copper adsorption on partially deacetylated prawn shell in batch systems have been obtained. The Langmuir model with pH-dependent parameters and the extended Langmuir–Freundlich model with pH-independent parameters adequately describe the equilibrium data. A diffusion-based model and two surface reaction rate models, a second order reversible reaction model and a second order irreversible reaction model, are used to describe the transient behavior of the batch contactor. The conformity of experimental uptake data with theoretical curves calculated from the diffusion model is rather poor. On the other hand, both reaction rate models can describe the kinetic profiles for copper adsorption over a range of C_0s and adsorbent dosage provided their rate constants are properly correlated with the two system variables. The best-fit values of the surface interaction rate constants are shown to increase with decreasing C_0 and increasing adsorbent dosage. These trends can be understood by considering the degree of metal loading on the adsorbent. The models clearly have the potential for use in the scaling up and design of batch adsorbers. It should however be noted that Langmuir parameters have been incorporated within the analytic solution for the second order reversible reaction model (Eq. (8)). Use of this expression is thus restricted to cases for which the adsorption equilibrium relationship is of the Langmuir type. In contrast, the analytic solution for the second order irreversible reaction model (Eq. (13)) is not limited by the type of adsorption isotherm expression.

References

[1] S.E. Bailey, T.J. Olin, R.M. Bricka, D.D. Adrian, Wat. Res. 33 (1999) 2469.
[2] R.W. Coughlin, M.R. Deshaies, E.M. Davis, Environ. Prog. 9 (1990) 35.
[3] V.W.D. Chui, K.W. Mok, C.Y. Ng, B.P. Luong, K.K. Ma, Environ. Int. 22 (1996) 463.
[4] M.Y. Lee, S.H. Lee, H.J. Shin, T. Kajiuchi, J.W. Yang, Process Biochem. 33 (1998) 749.
[5] R.L. Tseng, F.C. Wu, R.S. Juang, J. Environ. Sci. Health A34 (1999) 1815.
[6] I. Tsigos, A. Martinou, D. Kafetzopoulos, V. Bouriotis, Trends Biotechnol. 18 (2000) 305.
[7] S.T. Lee, F.L. Mi, Y.J. Shen, S.S. Shyu, Polymer 42 (2001) 1879.
[8] F.C. Wu, R.L. Tseng, R.S. Juang, Ind. Eng. Chem. Res. 38 (1999) 270.
[9] C. Huang, M.R. Liou, C.B. Liu, in: C.P. Huang (Ed.), Hazardous and Industrial Wastes, Technomic Publishing Company, Lancaster, 1994, p. 275.
[10] R. Bassi, S.O. Prasher, B.K. Simpson, Sep. Sci. Technol. 35 (2000) 547.
[11] R.S. Juang, F.C. Wu, R.L. Tseng, Wat. Res. 33 (1999) 2403.
[12] T.Y. Hsien, G.L. Rorrer, Ind. Eng. Chem. Res. 36 (1997) 3631.

[13] E. Guibal, C. Milot, J.M. Tobin, Ind. Eng. Chem. Res. 37 (1998) 1454.
[14] E. Guibal, A. Larkin, T. Vincent, J.M. Tobin, Ind. Eng. Chem. Res. 38 (1999) 4011.
[15] O.A.C. Monteiro Jr., C. Airoldi, J. Colloid Interf. Sci. 212 (1999) 212.
[16] C.L. Lasko, M.P. Hurst, Environ. Sci. Technol. 33 (1999) 3622.
[17] T. Becker, M. Schlaak, H. Strasdeit, React. Funct. Polym. 44 (2000) 289.
[18] F.C. Wu, R.L. Tseng, R.S. Juang, Wat. Res. 35 (2001) 613.
[19] T. Tianwei, H. Xiaojing, D. Weixia, J. Chem. Technol. Biotechnol. 76 (2001) 191.
[20] K.H. Chu, M.A. Hashim, J. Chem. Technol. Biotechnol. 75 (2000) 1054.
[21] L. Dambies, C. Guimon, S. Yiacoumi, E. Guibal, Colloids Surf. A 177 (2000) 203.
[22] D.D. Do, Adsorption Analysis: Equilibria and Kinetics, Imperial College Press, London, 1998.
[23] S. Yiacoumi, C. Tien, Kinetics of Metal Ion Adsorption from Aqueous Solutions: Models, Algorithms and Applications, Kluwer Academic Publishers, Norwell, 1995.
[24] G.I. Skidmore, H.A. Chase, in: M. Streat (Ed.), Ion Exchange for Industry, Ellis Horwood, Chichester, 1988, p. 520.
[25] E.H. Smith, Sep. Sci. Technol. 33 (1998) 149.
[26] J. Crank, The Mathematics of Diffusion, Oxford University Press, London, 1956.